Appendix: Methods and Results

1. Methods

A shear-wave traveling through an anisotropic medium is split into two perpendicular polarized shear waves that travel at different velocities (e.g., Crampin, 1985). From three-component seismic records, it is possible to extract: (1) the difference in arrival times (or delay time, δt) between the fast and slow shear-waves which is a function of the thickness and intrinsic anisotropy of the anisotropic medium; and (2) the orientation of the polarization planes of the fast shear wave (or the fast polarization direction, ϕ) which reflects the orientation of the structure. Teleseismic shear-wave XKS (including SKS, SKKS, PKS) are extensively employed in the study of deformation in the lithosphere and upper asthenosphere (e.g., Savage, 1999) due to several advantages as follows. First, the observed anisotropy can be localized to the receiver side of the path due to the longitudinal-wave (P wave) to shear-wave (S wave) conversion at the core-mantle boundary (CMB). Second, XKS phases are most easily observed beyond an epicentral distance of 85°. Third, XKS phases represent a nearly vertical ray path through the upper mantle and crust, so that lateral resolution is limited only by the station spacing and wavelengths used. Finally, although anisotropy measurement with XKS phases represent the vertically integrated effect of anisotropy from the CMB to the surface, seismological and petrophysical studies (e.g., Silver, 1996; Savage, 1999; Gung et al., 2003) indicate that the main source of anisotropy that causes splitting of XKS phases is located shallower than 400 km beneath a seismic station.

The XKS phases are initially radially polarized because they are longitudinal-wave (P wave) to shear-wave (S wave) converted phase from core-mantle boundary; consequently, when the original north-south and east-west components are rotated to the radial and transverse components, any XKS energy on the transverse component

indicates the existence of azimuthal anisotropy beneath the recording station (Silver, 1996). As is common in making splitting measurements, one search for the pair of splitting parameters ϕ (fast polarization direction) and δt (delay time) that, when used to correct for the anisotropy, most successfully removes XKS energy on the transverse component. To prevent systematic errors caused by uncorrected horizontal component misalignments, we measured the splitting parameters of each selected event by using the improved measurement method (Tian et al., 2011). During the measurements, the splitting analyses are repeated with different assumed angles of misalignment (typically ranging from -30° to 30°), and the corrected measurement of the splitting parameters obtained by meeting two criteria: (1) the horizontal rotating angle is found for the global minimum transverse energy using the minimum energy technique (hereafter SC; e.g., Silver and Chan, 1991), and (2) the results from the SC technique and the minimum eigenvalue technique (hereafter EV; e.g., Silver and Chan, 1991) are consistent. Figure S1 shows an example of the application this method. To suppress the potential effects on the splitting parameters caused by noise, all waveforms are band-pass filtered using a combination of corner frequencies 0.03 and 0.2 Hz. The master time windows used are about 16 s around the phase of interest based on the predicted travel times resulted from the IASP91 model (Kennett and Engdahl, 1991). The errors in the resulting splitting parameters can be calculated using the inverse F test and represent the 95% confidence level (Silver and Chan, 1991).

We consider a measurement devoid of energy on the transverse component of the seismogram as “null”. Null measurements may result from an absence of perceptible anisotropy or by initial shear wave polarization parallel to the fast or slow polarization direction in the anisotropy layer (e.g., Silver and Chan, 1991). In this study, only good measurements that satisfy the following conditions were used to constrain the final result: (1) the back-azimuth separation from the fast and slow polarization direction was larger

than 10°; (2) the 95% confidence regions of the estimated splitting parameters were small ($2\sigma_{\phi} < 22.5°$ and $2\sigma_{\delta t} < 1.0$ s). After measurement of the splitting parameter for each event, the station average was computed from the individual measurements weighted by the reciprocal of the variance obtained from the F test (Liu et al., 2008).

2. Splitting results

2.1 Parameters for a single-layer model

We obtained a total of 1326 pairs of good splitting parameters and 156 null measurements. Figure 2a presents the whole set of individual splitting measurements plotted at each respective station. Figure S2 plots the back azimuth of the events that produced null splitting measurements. Most individual measurements show an ENE-WSW or east-west or NW-SE fast polarization direction. Regionally, the fast polarization directions focus between ENE-WSW and east-west trending in the southeastern part of the map area (Fig. 2a), whereas most of the individual measurements in the northwestern part of the map area show east-west or NW-SE trending fast polarization direction. Figures 2c and 2e show that most fast polarization directions occur in the window 90±30°, while the delay times center on 1.2±0.2 s. Null back azimuths are consistent with these observations: most nulls are observed along the azimuths subparallel or perpendicular to the fast polarization direction (see Fig. S2). The station averages computed from the individual measurements are plotted in Figure 2b and listed in Table S1. Two averages are obtained if the fast directions from individual measurements at one station are distributed into two distinct groups (e.g, stations BAS, BEB, JIXah, and SIX). No average value is obtained if there are emanative fast polarization directions and few events used at the station. Figures 2d and 2f show average ϕ values between N070°E and N110°E and average δt close to 1.0 s at most stations. There are 15 stations with average fast polarization directions between N110°E and N150°E and 7 stations with average fast polarization directions between N050°E

and N070°E. Regionally, the average fast polarization directions in Figure 2b show a clockwise rotation between ENE-WSW to E-W in the southeastern part of the map area and NW-SE in the northwestern part.

For 5 stations, shear wave splitting results have been reported previously. At stations HEF, NJ2 and TIA, our average results are consistent with these results (Zhao et al., 2007; Chang et al., 2009). But at station LAY, Chang et al. (2009) reported results of 106.7 ± 7.8° and 0.92 ± 0.16 s for 5 events, whereas we obtained average values of 123.3 ± 22.5° and 0.93 ± 0.37 s for 25 events. Our averages at station CSH (58.7 ± 32.1°, 1.25 ± 0.32 s) obtained from 56 high-quality individual measurements are also somewhat inconsistent with the results (95.5 ± 9.9°, 1.05 ± 0.1 s) of Chang et al. (2009) using 5 events. These variations may have resulted from the use of a limited number of events.

2.2 Evidence for two layers of anisotropy

At stations CSH, ANQsd and NLA, we obtained a large number of measurements (56, 44 and 37, respectively) and large back-azimuth variations. Figure 3 shows the splitting parameters as a function of back-azimuth. These back-azimuth variations are clearly not random but rather are well organized. Such back-azimuth variations have been suggested to result from the presence of two anisotropic layers (Silver and Savage, 1994). Following the scheme proposed by these authors, we try to constrain the possible geometries of these anisotropic layers beneath the three stations.

For a dominant signal frequency of 0.125 Hz, we applied a forward approach by computing the apparent back-azimuth ϕ and δt variations for each two layer model by varying the fast directions in each layer in 2° steps (from 0° to 180°) and the delay time in steps of 0.1 s (from 0 to 2.6 s), producing a total of 5,904,900 models. To determine the

'best-fitting' model, we calculated a sum of squares of the two layer model misfit *SSd*:

$SSd = \Sigma(\phi_{observed} - \phi_{predicted})^2/\sigma_\phi^2 + \Sigma(\delta t_{observed} - \delta t_{predicted})^2/\sigma_{\delta t}^2$

Figure S2 shows an example for station CSH. Figure 3 shows the observed splitting parameters together with the best two layer model computed for each station. The best fitting models are listed in Table S3. Our results show a similar two layer model at all three stations. The fast direction in the upper layer is aligned ENE-WSW or east-west, whereas that of the lower layer is aligned NW-SE. The delay times in the upper layer show a large variation from 0.5 s to 1.1 s among the three stations, whereas the delay times of the lower layer show a small range from 1.2 s to 1.5 s.

We then use the statistical technique described in Walker et al. (2005) to judge the significance of the variance reduction over the best-fitting one layer mode. To estimate the degree to which a two layer model fits the splitting observations better than a single layer model with a horizontal fast axis, the goal of R^* is defined as a function of the misfit of two layer model (*SSd*) and the misfit of single layer model (*SSo*):

$R^* = 1-(N-1)/(N-k-1)*SSd/SSo$

where *N* is the number of data and *k* is the number of model parameters. The R* for the best fitting two layer model at the three stations are listed in Table S3. Walker et al. (2005) consider models that fit the data with $R^* > 0.25$ to be statistically significant. These results indicate that the two layer model significantly improves the fit with the observations at the three stations.

References Cited

Chang, L.J., Wang, C.Y., and Ding, Z.F., 2009, Seismic anisotropy of upper mantle in eastern China: Science in China Series D-Earth Sciences, v. 52, p. 774-783.

Crampin, S., 1985, Evaluation of anisotropy by shear-wave splitting: Geophysics, v. 50, p. 142-152.

Gung, Y., Panning, M., and Romanowicz, B., 2003, Global anisotropy and the thickness of continents: Nature, v. 422, p. 707-711.

Kennett, B.L.N., and Engdahl, E.R., 1991, Traveltimes for Global Earthquake Location and Phase Identification: Geophysical Journal International, v. 105, p. 429-465.

Liu, K.H., Gao, S.S., Gao, Y., and Wu, J., 2008, Shear wave splitting and mantle flow associated with the

deflected Pacific slab beneath northeast Asia: Journal of Geophysical Research-Solid Earth, v. 113, B01305, doi:10.1029/2007JB005178.

Savage, M.K., 1999, Seismic anisotropy and mantle deformation: what have we learned from shear wave splitting?: Reviews of Geophysics, v. 37, p. 65-106.

Silver, P.G., 1996, Seismic anisotropy beneath the continents: Probing the depths of geology: Annual Review of Earth and Planetary Sciences, v. 24, p. 385-432.

Silver, P.G., and Chan, W.W., 1991, Shear-Wave Splitting and Subcontinental Mantle Deformation: Journal of Geophysical Research-Solid Earth, v. 96, p. 16429-16454.

Silver, P.G., and Savage, M.K., 1994, The Interpretation of Shear-Wave Splitting Parameters in the Presence of 2 Anisotropic Layers: Geophysical Journal International, v. 119, p. 949-963.

Tian, X.B., Zhang, J.L., Si, S.K., Wang, J.B., Chen, Y., and Zhang, Z.J., 2011, SKS splitting measurements with horizontal component misalignment: Geophysical Journal International, v. 185, p. 329-340.

Walker, K.T., Bokelmann, G.H.R., Klemperer, S.L., and Bock, G., 2005, Shear-wave splitting around the Eifel hotspot: evidence for a mantle upwelling: Geophysical Journal International, v. 163, p. 962-980.

Zhao, L., Zheng, T.Y., Chen, L., and Tang, Q.S., 2007, Shear wave splitting in eastern and central China: Implications for upper mantle deformation beneath continental margin: Physics of the Earth and Planetary Interiors, v. 162, p. 73-84.

Figure S1. Example of a SKS splitting using the improved measurement method (Tian et al., 2011) for event 20080523.193534 at station CSH. (a) The original seismogram after rotating the north and east components by 1° counter-clockwise to represent misalignment. The left panel shows the radial (bold line) and transverse (gray thin line) components and the time window (vertical dash lines) of the PKS phase analyzed. The right panel shows the initial particle motion. (b) The measurement of splitting parameters by the SC method. The left panel is the contour map of the energy on the transverse component with the best-fitting splitting parameters shown with the cross. The middle panel shows the corrected radial (bold line) and transverse (gray thin line) component, and the right panel is the corrected particle motion. (c) same as (b) but using the RC method. The contour map shows the correlation coefficient. The bold line and the gray thin line in middle panel are the corrected fast and slow components, respectively. (d) same as (c) but using the EV method. The contour map shows the minimum eigenvalue.

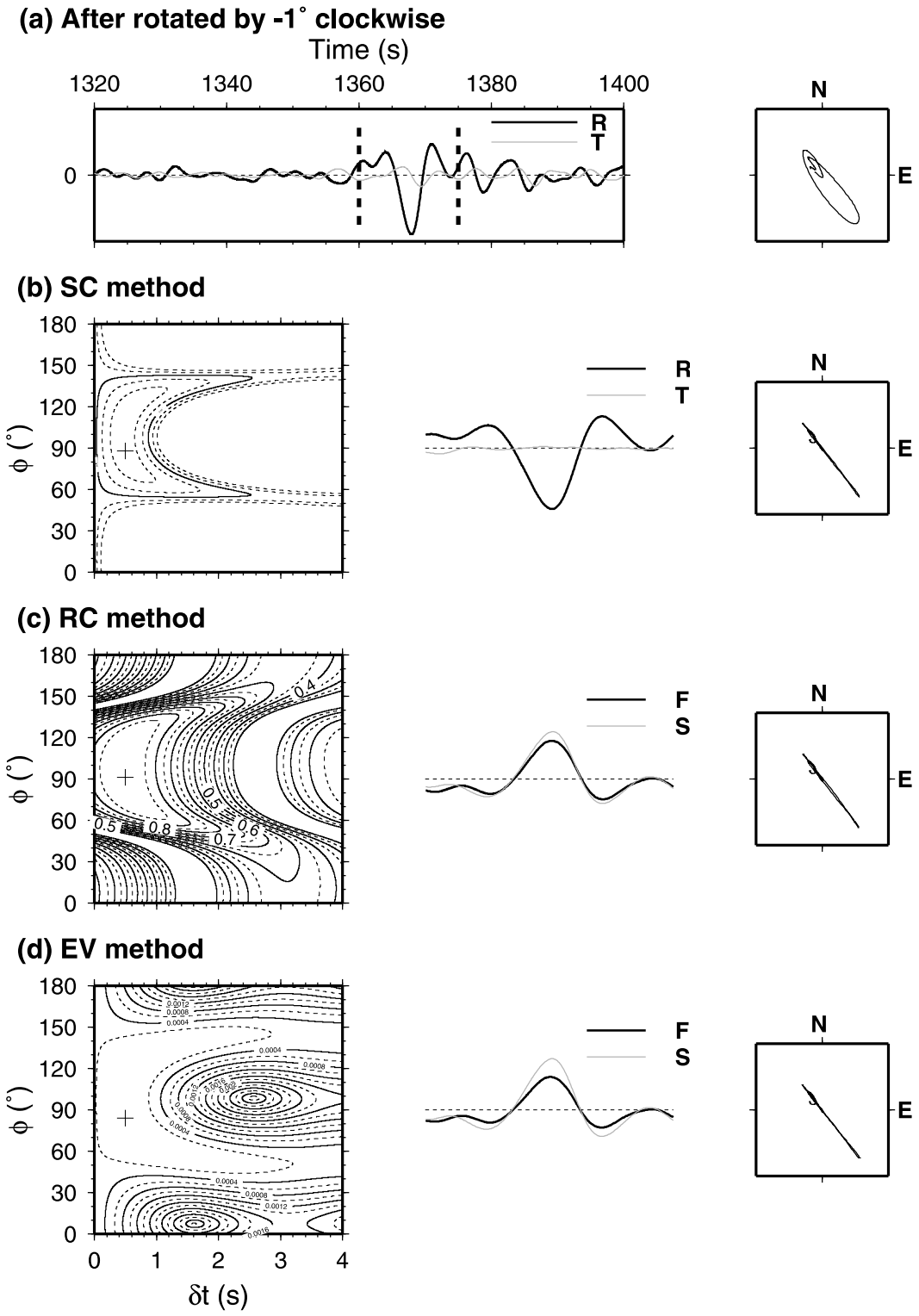
(a) After rotated by -1˚ clockwise
Time (s)
1320
1340
1360
1380
1400
0
R
T
N
E
(b) SC method
180
150
120
90
60
30
0
ϕ (˚)
R
T
N
E
(c) RC method
0.4
0.5
0.6
0.7
0.8
0.5
F
S
N
E
(d) EV method
0.0004
0.0008
0.0012
F
S
N
E
0
1
2
3
4
δt (s)

Figure S1

Figure S2. Null measurements observed at each station. Directions of each segment represent the back azimuth of the events that produced nulls.

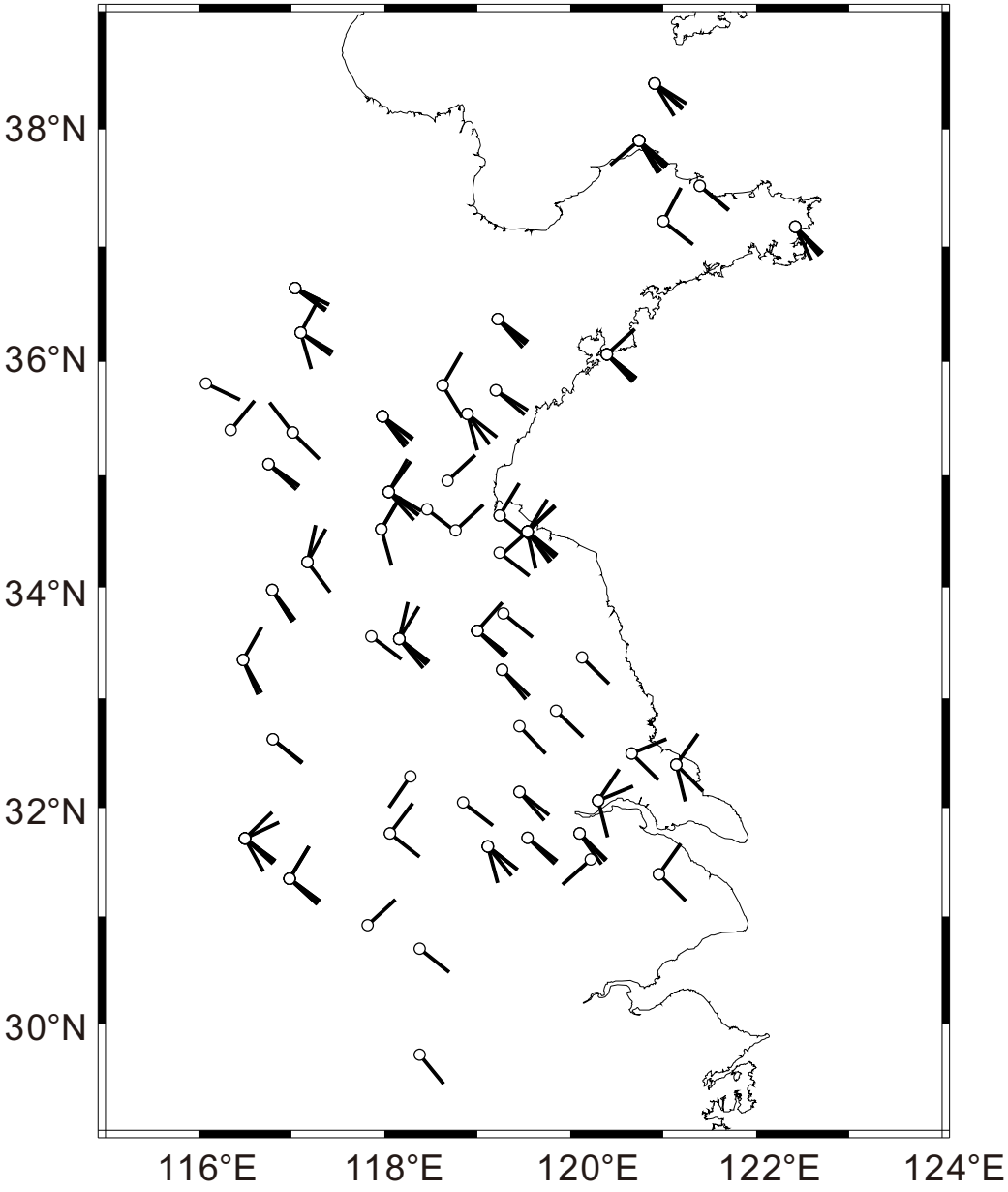

Figure S2

Figure S3. Two layer anisotropy fitting at station CSH. (a) and (b) show apparent variations of the splitting parameters (black circle with error bar) as a function of the back-azimuth of the incoming wave, together with the best fitting two layer model (blue line). (c) the polar plot shows individual splitting measurements with back azimuth (angle) and (radius). The orientation of line is parallel to the fast direction and its length is proportional to the delay time. The histograms in (d) and (e) show the statistical distribution of the upper and lower fast directions of the 1000 best two layer models. (f) The statistical distribution of the fast directions of upper (red lines) and lower (blue lines) layers in the 1000 best models in each bootstrap resampling and fitting procedure. (g) The distribution of parameters of the best two layer models of each bootstrap resampling and fitting procedures. Red and blue points represent the upper and lower layer, respectively. The mean values of parameters are shown as open diamonds and STD are shown as error bars.

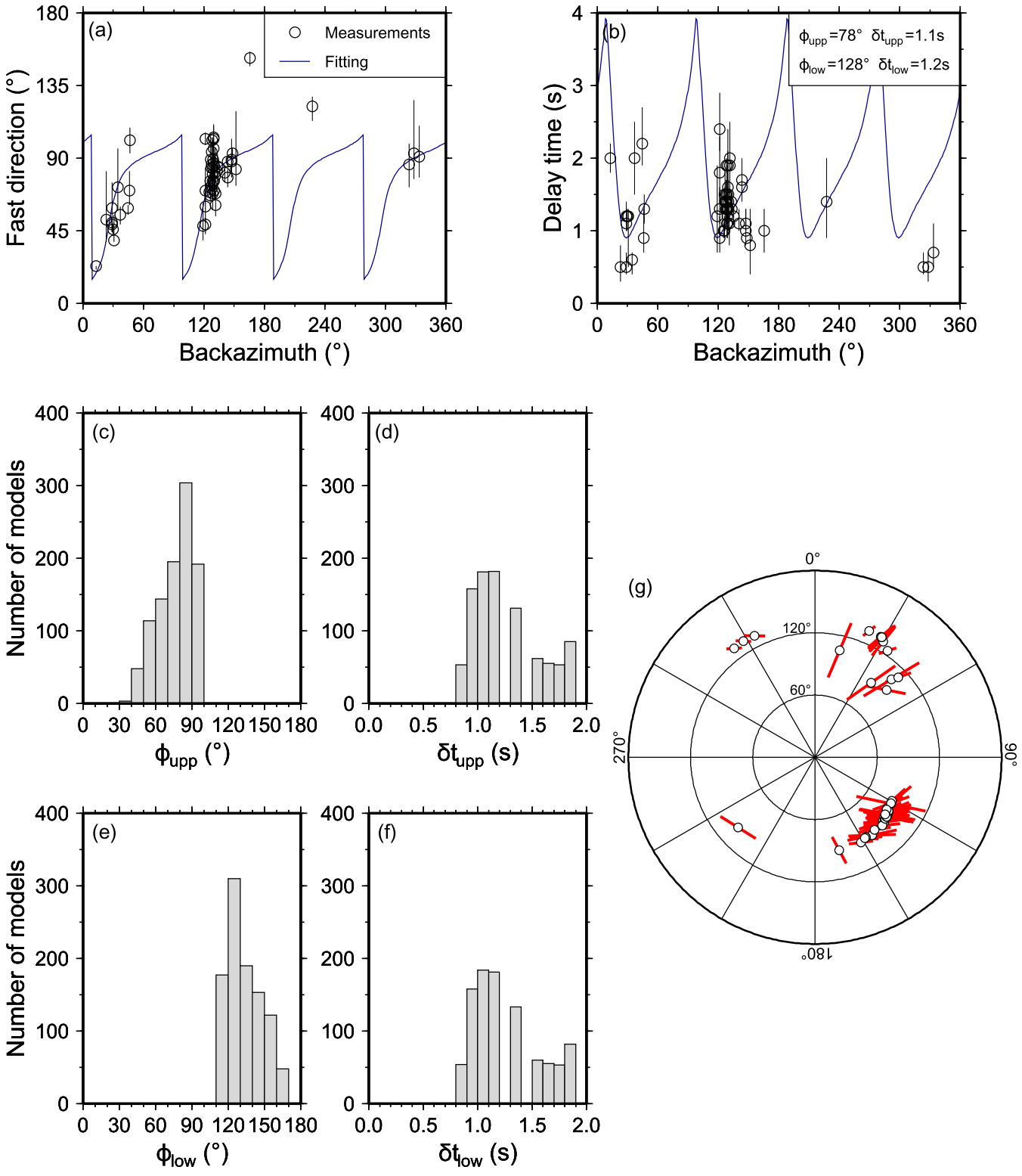
(a)
Measurements
Fitting
Fast direction (°)
Backazimuth (°)
(b)
ϕ_{upp}=78° δt_{upp}=1.1s
ϕ_{low}=128° δt_{low}=1.2s
Delay time (s)
Backazimuth (°)
(c)
(d)
(e)
(f)
Number of models
ϕ_{upp} (°)
δt_{upp} (s)
ϕ_{low} (°)
δt_{low} (s)
(g)
0°
90°
180°
270°
60°
120°

Figure S3

Table S1. Station Locations and the Averaged Splitting Parameters Values

Station	Longitude (°E)	Latitude (°N)	Elevation (m)	ϕ (°)	dϕ (°)	δt (s)	dδt (s)	Number of Measurements
ANQah	117.02	30.58	75	86.4	16.9	1.01	0.35	12
BAS	117.38	31.47	45	69.8	16	0.86	0.19	11
				140.2	19.5	1.17	0.2	3
BEB	117.3	32.91	40	27	6.4	1.23	0.57	2
				139.8	2.8	1.7	0.61	4
BZY	116.22	31.4	189	90.1	10.5	1.05	0.16	4
CHZ	118.28	32.29	112	45.4	29.5	0.83	0.32	8
DYN	117.47	32.64	196	158.2	13.4	0.83	0.19	6
FZL	116.27	31.35	90	86.6	39.2	0.92	0.22	14
HBE	116.79	33.98	90	98.7	13.8	1.6	0.27	31
HEF	117.14	31.82	77	124.7	25.2	1.36	0.32	15
HNA	116.8	32.63	86	130.9	20.1	1.33	0.5	17
HSH	118.06	31.77	181	74.8	28	1.18	0.45	3
HUS	118.38	29.71	130	84.3	16.3	1.19	0.23	7
JAS	118.26	32.81	95	102.2	24.8	0.72	0.31	3
JIXah	118.38	30.7	55	75.4	7.2	1.12	0.22	10
				133.1	4.2	1.48	0.24	3
JZA	115.88	31.69	50	105.4	13.2	0.98	0.41	9
LAN	116.5	31.72	60	104	22.8	1.15	0.25	4
LNA	117.14	31.34	245	77.6	15	0.87	0.21	3
MAS	118.57	31.69	33	80.6	24.5	1.41	0.31	12
MCG	116.48	33.35	55	109	11.2	1.31	0.65	11
SCH	116.98	31.35	65	109	29.7	1.26	0.35	2
SIX	117.86	33.56	42	75.1	8.5	1.03	0.15	6
				172.7	10.9	1.09	0.19	10
SJH	116.09	31.44	240	94.4	4.6	1.16	0.14	3
TOL	117.82	30.92	49	111.3	38.8	1.03	0.32	17
BY	119.27	33.26	-500	57.3	12.6	1.33	0.54	6
CS	120.71	31.67	27	87.7	9.7	1.03	0.28	4
CZ	120.1	31.77	106	87.7	9.7	1.03	0.28	1
DH	118.77	34.51	30	84.2	20.1	1.09	0.28	16
GAY	118.98	34.94	65	86.8	16.9	1.45	0.28	14
GC	119.02	31.35	50	120.3	55.8	1.07	0.39	9
GUY	119.24	34.31	43	75.9	17.6	0.89	0.31	11
JT	119.54	31.73	80	76.6	12.7	1.18	0.45	6
LH	118.94	32.51	104	56.9	32.8	1.32	0.42	9
LIS	119.11	31.65	36	70.7	19.5	1.04	0.59	3
LYG	119.24	34.64	40	69.4	4.8	1.21	0.59	3
NJ2	118.85	32.05	45	89.7	5.1	1.29	0.05	3
NT	120.89	31.95	-105	66.6	15.2	1.31	0.23	3
PX	116.9	34.8	-370	98.4	17.1	1.36	0.2	10
PZ	117.97	34.52	50	98	11.7	1.34	0.35	14
QSD	119.82	35	23	122.1	2.1	2.03	0.85	2
TZ	119.92	32.41	-490	86.7	4.2	1.16	0.48	4
XW	119.54	34.5	45	107.9	12.5	1.05	0.2	5
XY	118.49	33	40	108.2	13.6	0.95	0.44	4

XZ	117.17	34.23	62	96.5	20.2	1.5	0.2	16
YC	120.13	33.37	-400	95.1	7.1	1.02	0.14	2
ZJ	119.45	32.15	34	89.8	12.2	1.26	0.26	5
ANQsd	119.22	36.37	100	93	30.2	1.33	0.3	44
BHC	120.91	38.39	54	79.6	7.5	1.41	0.4	18
CSH	118.05	34.85	65	58.7	32.1	1.25	0.32	56
DSD	116.75	35.1	72	98.6	5.7	1.86	0.3	19
DSH	117.67	38	42	115	23.9	0.89	0.19	9
HAY	121.32	36.82	79	75.3	25	0.97	0.35	26
JIN	117.04	36.64	131	141.6	37.3	1	0.47	24
JIXsd	116.35	35.4	108	119	19	0.92	0.41	28
JUN	118.85	35.17	134	82.4	12.4	1.28	0.37	35
JUX	118.89	35.54	149	90.3	24.6	1.23	0.37	34
LAS	119.32	35.13	111	98.6	10.9	1.48	0.21	17
LAY	120.72	36.99	77	123.3	22.5	0.93	0.37	25
LIS	118.68	34.95	192	78.6	12.5	1.49	0.25	19
LOK	120.51	37.55	168	98.6	34.7	1.13	0.28	21
LQU	118.49	36.41	208	107	16.2	1.07	0.39	17
LSH	116.08	35.81	60	109.5	6.6	1.01	0.66	23
LZH	121	37.22	239	127.3	12.2	0.71	0.42	14
NLA	117.98	35.52	267	106.6	26.5	1.4	0.39	37
QID	120.39	36.06	14	55.2	9.9	1.34	0.45	12
RCH	122.42	37.17	64	91.8	23.4	1.26	0.4	21
RSH	121.6	36.92	98	82.7	14	1.03	0.22	11
RZH	119.52	35.42	880	75.3	32.8	0.99	0.3	17
TCH	118.46	34.7	110	75.8	8.3	1.41	0.44	25
TIA	117.1	36.25	300	119.6	27.8	0.73	0.57	28
WED	121.92	37.18	99	83.3	18	0.96	0.4	13
WUL	119.2	35.75	152	100.8	26.6	0.91	0.4	33
XIT	117.76	35.95	280	76.6	31.1	1.14	0.32	13
YSH	118.63	35.79	174	80.9	39.1	1.13	0.21	23
YTA	121.39	37.52	20	144	28.4	0.96	0.53	6
ZCH	117.01	35.38	138	76.3	32.9	1.04	0.29	44

Table S2. Selected Events

Date	Time	Latitude (°N)	Longitude (°E)	Depth (km)	Mag.	Observation No.
2007.08.20	22:42:28	8.04	-39.25	6	6.5	2
2007.08.27	5:37:56	-25.73	179.61	497	5.4	1
2007.09.10	1:49:11	2.97	-77.96	15	6.8	17
2007.09.25	5:16:01	-30.97	180	416	6.2	27
2007.09.30	5:23:34	-49.27	164.12	10	7.4	11
2007.09.30	9:47:51	-49.14	164.11	18	6.6	7
2007.10.05	7:17:52	-25.19	179.46	509	6.5	2
2007.10.15	12:29:34	-44.8	167.55	18	6.8	17
2007.10.15	21:28:23	-44.79	167.46	19	6.1	22
2007.10.16	8:41:45	-33.03	-178.32	39	5.4	17
2007.10.16	21:05:43	-25.77	179.53	509	6.6	3
2007.11.02	22:31:43	-55.47	-128.97	10	6.1	15
2007.11.10	1:13:29	-51.78	161.32	10	6.6	1
2007.11.16	3:13:00	-2.31	-77.84	122	6.8	1
2007.12.09	7:28:20	-26	-177.51	152	7.8	9
2007.12.20	7:55:15	-39.01	178.29	20	6.6	35
2008.02.03	7:34:12	-2.3	28.9	10	5.9	2
2008.02.08	9:38:14	10.67	-41.9	9	6.9	2
2008.02.12	12:50:18	16.36	-94.3	83	6.5	3
2008.02.21	14:16:02	41.15	-114.87	6	6	16
2008.03.01	23:06:44	-35.38	-179.3	24	5.6	3
2008.03.13	13:28:44	-45.49	35.01	10	6	2
2008.03.14	16:02:22	-22.25	-175.04	35	5.4	1
2008.03.18	8:22:47	-29.25	-177.44	25	6.2	15
2008.03.28	6:39:47	-32.88	179.36	365	5.7	3
2008.04.12	0:30:12	-55.66	158.45	16	7.1	2
2008.04.15	3:03:04	13.56	-90.6	33	6.1	18
2008.04.26	23:34:49	-49.09	164.12	10	6.1	25
2008.05.16	11:06:50	-32.54	-178.36	35	5.4	3
2008.05.23	19:35:34	7.31	-34.9	8	6.5	15
2008.05.27	5:51:12	-56.6	147.41	10	5.9	8
2008.06.25	2:41:43	-56.01	-143.68	10	5.3	1
2008.06.26	21:19:15	-20.77	-173.34	38	6.2	6
2008.07.03	6:34:53	10.28	-60.44	33	5.8	7
2008.07.16	17:09:19	-31.13	-178.51	89	5.5	13
2008.07.23	8:12:40	-67.14	112.22	10	5.3	1
2008.08.09	6:01:48	-60.65	153.77	10	6.5	1
2008.08.27	6:46:19	-10.75	41.47	10	5.7	1
2008.09.01	4:00:39	-25.39	-177.64	171	6	18
2008.09.04	16:09:51	-31.56	-177.81	26	5.8	36
2008.09.10	13:08:14	8.09	-38.71	9	6.6	12
2008.09.29	15:19:31	-29.76	-177.68	36	7	4
2008.10.02	13:03:08	-30.78	-178.13	92	5.4	15
2008.10.04	14:50:30	-30.43	-177.25	36	5.3	3
2008.10.05	9:12:36	-30.18	-177.18	10	6.1	30
2008.10.11	12:23:29	-29.82	-176.9	35	5.5	1

2008.10.19	5:10:33	-21.86	-173.82	29	6.9	10
2008.10.19	12:55:05	-21.97	-173.7	35	5.6	3
2008.11.02	15:00:55	-29.92	-176.96	10	5.7	24
2008.11.06	9:11:05	-29.85	-177.44	19	5.9	9
2008.11.19	6:11:20	8.27	-82.97	32	6.3	4
2008.12.08	18:39:09	-53.01	106.82	11	6.3	4
2008.12.09	6:23:59	-31.23	-176.92	18	6.8	39
2008.12.13	8:45:36	-48.98	123.4	10	5.9	1
2009.01.18	14:11:48	-30.2	-177.95	33	6.4	7
2009.01.24	1:28:39	-28.25	-176.7	10	6	1
2009.02.12	18:54:28	-31.23	-178.11	23	5.9	5
2009.02.17	3:30:53	-30.72	-178.62	13	6	1
2009.02.18	21:53:45	-27.42	-176.33	25	6.9	27
2009.02.28	14:33:06	-60.53	-24.8	15	6.3	1
2009.03.11	17:24:36	8.5	-83.22	14	5.9	8
2009.03.11	21:03:58	8.49	-83.21	17	5.9	8
2009.03.12	23:23:34	5.69	-82.77	9	6.3	1
2009.04.04	11:07:12	-22.51	-174.66	35	5.5	8
2009.04.16	14:57:06	-60.2	-26.86	20	6.7	2
2009.04.18	2:03:52	-28.92	-177.45	65	5.8	7
2009.04.26	0:06:53	-30.3	-178.58	131	6.1	24
2009.05.03	16:21:47	14.57	-91.17	123	6.2	3
2009.05.10	1:16:06	1.39	-85.17	6	6.1	1
2009.05.16	0:53:52	-31.52	-178.79	54	6.5	2
2009.05.24	0:58:02	-31.48	-177.68	4	6	3
2009.06.09	22:42:38	-55.06	-126.65	10	5.6	4
2009.06.16	20:05:56	-54.37	5.87	10	6.1	5
2009.07.04	6:49:35	9.59	-78.97	38	6	8
2009.07.15	9:22:29	-45.76	166.56	12	7.8	4
2009.07.30	20:05:34	-20.85	-174.25	10	5.8	2
2009.08.05	8:31:40	-45.55	166.36	10	6.1	36
2009.08.13	3:46:53	-26.76	-114.26	10	5.3	1
2009.08.18	21:20:47	-26.06	-178.39	269	6.3	19
2009.09.02	18:00:11	-29.35	-178.96	275	6.2	28
2009.09.12	20:06:24	10.7	-67.92	10	6.3	18
2009.09.24	7:16:24	18.98	-107.37	37	6.3	28
2009.10.02	22:38:38	-17.79	-172.76	11	5.4	1
2011.01.24	1:13:01	-19.2	-173.51	16	5.7	1
2011.02.00	6:14:16	-22.01	-175.62	76	6	3
2011.02.21	11:07:49	-26.14	178.39	558	6.5	3
2011.02.22	0:02:56	-43.58	172.68	6	6.1	42
2011.02.25	13:20:42	17.84	-95.01	123	5.9	1
2011.03.06	14:47:46	-56.42	-27.06	88	6.5	2
2011.03.20	15:31:02	-31.13	-179.82	321	5.7	1
2011.04.07	13:24:17	17.21	-94.34	166	6.6	17
2011.04.14	21:04:30	11.17	-86.35	35	5.7	11
2011.04.18	13:13:52	-34.34	179.87	86	6.6	68
2011.05.05	16:25:59	-25.19	-177.55	185	5.6	1
2011.05.09	19:06:07	-56.65	147.41	9	5.9	21
2011.05.10	15:19:34	-4.74	-105.59	10	5.5	31

2011.05.13	23:02:05	9.95	-84.31	73	5.9	14
2011.05.15	13:22:39	0.57	-25.65	10	6.1	1
2011.05.21	21:27:58	-30.82	-178.17	34	5.9	32
2011.06.05	12:02:31	-55.84	146.62	3	6.4	24
2011.06.09	20:27:27	-30.42	-178.05	31	5.6	1
2011.06.13	2:32:01	-43.56	172.74	6	5.9	39
2011.07.07	9:21:49	-28.98	-176.71	10	5.7	39
2011.07.07	9:41:06	-29.15	-176.94	31	5.8	9
2011.07.09	14:05:24	-29.39	-177.12	19	5.9	23
2011.07.09	19:46:26	-29.44	-177.01	15	6	12
2011.07.11	7:26:41	-29.49	-176.58	11	5.9	43
2011.07.11	10:59:29	-22.68	-174.75	21	5.6	4
2011.07.16	7:14:29	-22.43	-175	7	5.8	13
2011.07.27	23:14:49	10.8	-43.39	10	5.9	2
2011.08.05	16:19:56	-29.99	-176.73	10	5.7	20
2011.08.20	1:35:57	-22.5	-174.94	10	5.6	6
2011.08.22	9:49:35	-29.03	-176.68	10	5.7	47
2011.08.23	18:03:24	37.94	-77.93	6	5.8	23
2011.08.24	18:03:58	-7.64	-74.53	147	7	2
2011.09.03	5:04:08	-56.45	-26.85	84	6.4	2
2011.09.09	19:37:29	-49.59	164.01	10	5.9	4
2011.09.14	13:47:40	-35.11	-178.99	13	5.7	51
2011.10.07	9:09:44	-32.51	-179.04	36	6.1	1
2011.10.08	9:04:08	-20.6	-173.22	6	5.9	7
2011.10.28	11:18:13	-28.78	-176.12	50	5.7	1
2011.11.02	15:13:44	-55.29	-128.84	10	6.1	13
2011.11.07	22:49:23	11.56	-85.86	177	6	9
2011.11.18	8:02:48	-37.81	179.42	12	5.8	9
2011.12.11	2:00:39	17.84	-99.96	54	6.5	1
2011.12.11	10:12:40	-56.01	-28.18	116	6.2	2
2011.12.15	10:21:21	-32.72	-179.1	32	6	1
2011.12.19	5:43:28	-29.07	-176.86	10	5.7	3
2011.12.23	2:29:21	-43.53	172.74	7	5.9	7
2011.12.23	11:03:26	-33.81	-178.34	10	5.5	6
2012.01.28	17:53:58	-29.43	-177.39	21	5.9	2
2012.02.09	19:04:39	-58.31	157.84	10	5.9	1
2012.02.13	11:09:27	9.18	-84.12	16	5.9	28
2012.03.20	18:16:07	16.49	-98.23	20	7.4	5
2012.04.12	7:18:18	28.84	-113.03	9	6	2
2012.04.12	7:27:52	28.7	-113.1	13	7	5
2012.04.17	19:18:48	-59.02	-16.61	12	6.2	17
2012.04.22	13:22:34	-52.87	140.29	12	5.6	1
2012.04.23	17:47:03	-28.56	-177.41	114	6	53
2012.04.28	10:18:47	-18.68	-174.71	135	6.6	1
2012.05.02	12:29:14	-54.56	143.84	10	5.8	15
2012.05.05	20:34:29	-21.48	-174.23	9	5.7	4
2012.05.23	23:10:52	-50.42	139.52	10	6	4
2012.05.28	21:57:39	-19.96	-175.98	211	5.9	1
2012.06.04	0:59:43	5.3	-82.63	7	6.3	7
2012.06.22	2:31:25	-32.94	-178.65	14	5.5	1

2012.06.22	4:42:45	-54.36	158.79	14	5.7	2
2012.06.29	15:46:15	-24.75	-9.66	10	5.8	2
2012.07.03	10:46:52	-40.02	173.76	230	6.3	36
2012.07.11	11:23:31	-26.05	-177.36	90	5.7	2
2012.07.21	5:05:18	-37.71	-179.97	12	5.6	50
2012.08.26	11:35:06	-65.48	-179.78	10	5.6	1
2012.09.05	14:56:25	10.09	-85.32	35	7.6	4
2012.09.06	23:47:33	-4.6	-105.89	10	5.7	2
2012.09.08	20:43:45	10.08	-85.32	35	5.7	19
2012.09.25	23:57:34	24.67	-110.17	10	6.3	33
2012.10.00	16:46:04	1.93	-76.36	170	7.3	3
2012.10.09	12:43:53	-60.33	153.7	10	6.6	1
2012.10.24	0:59:33	10.09	-85.3	17	6.5	1
2012.10.24	0:59:50	10.09	-85.3	17	6.5	23
2012.10.24	1:00:00	10.09	-85.3	17	6.5	2
2012.10.24	1:00:01	10.09	-85.3	17	6.5	1
2012.10.24	1:00:03	10.09	-85.3	17	6.5	1
2012.10.24	1:00:04	10.09	-85.3	17	6.5	1
2012.10.24	1:00:05	10.09	-85.3	17	6.5	1
2012.10.24	1:00:06	10.09	-85.3	17	6.5	1
2012.10.24	1:00:09	10.09	-85.3	17	6.5	1
2012.11.07	16:49:21	13.96	-91.85	24	7.4	10
2012.11.17	5:23:55	-18.38	-172.32	10	5.9	4
2012.12.07	18:29:54	-38.47	176.1	163	6.3	24
2012.12.14	10:47:27	31.09	-119.66	13	6.3	36
2013.02.09	14:30:43	1.14	-77.4	145	6.9	4
2013.02.15	3:13:11	-19.73	-174.46	74	5.7	2
2013.02.18	16:43:52	-30.73	-178.14	54	5.5	1
2013.02.24	21:05:14	-32.18	-178.06	10	5.5	15
2013.03.19	3:44:09	-58.92	-24.41	31	5.9	2
2013.03.22	22:52:03	-28.04	-176.57	12	5.5	1
2013.04.02	14:46:47	-40.46	45.36	9	5.9	1
2013.04.02	14:46:50	-40.46	45.36	9	5.9	1
2013.04.02	14:46:54	-40.46	45.36	9	5.9	1
2013.04.02	14:46:55	-40.46	45.36	9	5.9	1
2013.04.02	14:46:56	-40.46	45.36	9	5.9	2
2013.04.02	14:46:57	-40.46	45.36	9	5.9	3
2013.04.02	14:46:58	-40.46	45.36	9	5.9	1
2013.04.02	14:46:59	-40.46	45.36	9	5.9	1
2013.04.02	14:47:00	-40.46	45.36	9	5.9	1
2013.04.02	14:47:02	-40.46	45.36	9	5.9	1
2013.04.02	14:47:03	-40.46	45.36	9	5.9	3
2013.04.02	14:47:04	-40.46	45.36	9	5.9	2
2013.04.02	14:47:05	-40.46	45.36	9	5.9	2
2013.04.02	14:47:06	-40.46	45.36	9	5.9	3
2013.04.02	14:47:07	-40.46	45.36	9	5.9	2
2013.04.02	14:47:09	-40.46	45.36	9	5.9	1
2013.04.02	14:47:12	-40.46	45.36	9	5.9	1
2013.04.02	14:47:16	-40.46	45.36	9	5.9	1
2013.04.02	14:47:18	-40.46	45.36	9	5.9	1

2013.04.26	7:03:44	-28.74	-178.92	349	6.2	1
2013.04.26	7:03:45	-28.74	-178.92	349	6.2	1
2013.04.26	7:03:46	-28.74	-178.92	349	6.2	2
2013.04.26	7:03:47	-28.74	-178.92	349	6.2	5
2013.04.26	7:03:48	-28.74	-178.92	349	6.2	4
2013.04.26	7:03:49	-28.74	-178.92	349	6.2	3
2013.04.26	7:03:50	-28.74	-178.92	349	6.2	7
2013.04.26	7:03:51	-28.74	-178.92	349	6.2	6
2013.04.26	7:03:52	-28.74	-178.92	349	6.2	5
2013.04.26	7:03:53	-28.74	-178.92	349	6.2	3
2013.04.26	7:03:54	-28.74	-178.92	349	6.2	2
2013.04.26	7:03:55	-28.74	-178.92	349	6.2	7
2013.04.26	7:03:56	-28.74	-178.92	349	6.2	2
2013.04.26	7:03:57	-28.74	-178.92	349	6.2	2
2013.04.26	7:03:59	-28.74	-178.92	349	6.2	2
2013.04.26	7:04:01	-28.74	-178.92	349	6.2	2
2013.04.26	7:04:02	-28.74	-178.92	349	6.2	1
2013.04.26	7:04:03	-28.74	-178.92	349	6.2	1
2013.04.26	7:04:04	-28.74	-178.92	349	6.2	1

Table S3. Splitting Parameter Valus of the Best Two Layer Models

Station	Latitude (°)	Longitude (°)	ϕ_{upp} (°)	δt_{upp} (s)	ϕ_{low} (°)	δt_{low} (s)	R*
CSH	34.85	118.05	78	1.1	128	1.2	0.55
ANQsd	36.37	119.22	92	0.5	124	1.5	0.78
NLA	35.52	117.98	94	1	130	1.4	0.27